Scientific Research Publishing

World Journal of Engineering and Technology, 2025, 13(3), 514-535
https://www.scirp.org/journal/wjet
ISSN Online: 2331-4249
ISSN Print: 2331-4222

Validation of Neutronic and Thermal Hydraulic Parameters Displayed by the Ghana Research Reactor-1 Control System

Charlotte Anima Nketia[1], Edward Oscar Amponsah-Abu[1,2], Henry Cecil Odoi[1,2], Kwame Gyamfi[1,2], Isaac Kwasi Baidoo[1,2], Edward Shitsi[1,2,3*]

[1]Graduate School of Nuclear and Allied Sciences, University of Ghana, Accra, Ghana
[2]Nuclear Reactors Research Centre, National Nuclear Research Institute, Ghana Atomic Energy Commission, Accra, Ghana
[3]Nuclear Energy Planning Centre, Nuclear Power Institute, Ghana Atomic Energy Commission, Accra, Ghana
Email: canimanketia@gmail.com, edwardabu2002@yahoo.com, hencilod@gmail.com, kingbascillus@yahoo.co.uk, baidooisaac51@yahoo.co.uk, *edwardshitsi@yahoo.com

How to cite this paper: Nketia, C.A., Amponsah-Abu, E.O., Odoi, H.C., Gyamfi, K., Baidoo, I.K. and Shitsi, E. (2025) Validation of Neutronic and Thermal Hydraulic Parameters Displayed by the Ghana Research Reactor-1 Control System. *World Journal of Engineering and Technology*, **13**, 514-535.
https://doi.org/10.4236/wjet.2025.133034

Received: June 6, 2025
Accepted: August 5, 2025
Published: August 8, 2025

Abstract

The accuracy of neutronic and thermal hydraulic measurement values displayed by the Ghana Research Reactor-1 (GHARR-1) control system was investigated. The reactor core underwent a conversion from High Enriched Uranium (HEU) to low Enriched Uranium (LEU). After five (5) years of operation with the new LEU core, it is necessary to validate the core parameters of the reactor to ascertain its safety for continuous operation. The conversion of GHARR-1 core from HEU to LEU caused changes in the fuel composition, which could affect reactor core parameters during operation. Hence, the neutronic and thermal-hydraulic parameters displayed by the micro-computer control system need to be validated to ascertain their reliability for experiments after 5 years of operation. The validation of the authenticity of measurements made by the GHARR-1 control system was done using the Micro Computer Closed Loop System (MCCLS). The findings demonstrated that the pre-set neutron fluxes at the control systems are 1.08 times higher than the neutron fluxes obtained using a flux monitor (cobalt) at the inner irradiation site of the reactor when the reactor is operated at different power levels of 0.17 W - 34 kW using one micro-fission chamber. The obtained fluxes' average percentage deviations from the pre-set range (5.0×10^9 to 1.0×10^{12} ncm^{-2}s^{-1}) were 5.3%. When operating the reactor at the critical neutron flux of 5.0×10^9 ncm^{-2}s^{-1}, the core excess reactivity decreased by 7% of its nominal value of 3.87 mk. The inlet temperatures and the temperature difference across the reactor core were used to predict power levels. Results obtained show a variation in the experimental

power levels as compared with the pre-set power levels giving a mean variation of 5.8%. Thus, there is agreement between the values of the neutronic parameters (pre-set power levels) displayed by the Ghana Research Reactor-1 control system and that of the experimental values determined using flux monitor and thermal-hydraulic parameters (inlet temperature and the temperature difference across the reactor core). Otherwise, appropriate reactor calibration activities and/or addition of beryllium shim to maintain the neutron flux economy for detection have to be carried out to ensure the safety of the research reactor operation.

Keywords

Neutron Activation Analysis, Low Enriched Uranium, Neutron Flux, Temperature, Reactor Power

1. Introduction

The Ghana Research Reactor-1 (GHARR-1) was purchased through a tripartite arrangement between Ghana, China, and the International Atomic Energy Agency (IAEA). It is a commercialized version of the prototype Chinese Miniature Neutron Source Reactor (MNSR) (Amuasi *et al.* [1]). It was installed in December 1994 and operated on fuel containing 90.2% High Enriched Uranium (HEU) fuel.

In August 2017, the fuel of the reactor was changed from High Enriched Uranium (HEU) to Low Enriched Uranium (LEU) in order to meet the objectives of the Treaty on the Non-Proliferation of Nuclear Weapons (NPT) and lessen associated security implications, wrongful use of civil nuclear application and proliferation risks. The reactor, after completion of the conversion in August 2017, runs at a nominal power of 34 kW with 13.0% LEU fuel that corresponds to a thermal neutron flux of 1×10^{12} n/cm^2·s. The reactor is a tank-in-pool type that uses Uranium Aluminium Alloy (UAl_4) in an Aluminium (Al) matrix as fuel, light water as a moderator, coolant, and beryllium as a reflector. The reactor is cooled by natural convection. Figure 1 shows the vertical cross section of the GHARR-1 Reactor.

GHARR-1 is controlled by two separate control systems: a Control Console (CC) and a Micro Computer Closed-loop System (MCCLS) running the Windows operating system "eXPerience" (Win XP) (Amponsah-Abu [3]). The reactor is mainly used for Neutron Activation Analysis (NAA) and research, and human resource development for nuclear power projects (Amoah *et al.* [4]; Amponsah-Abu *et al.* [5]; Baidoo *et al.* [6]; Osei [7]; Osei *et al.* [8]).

The main objective of the study is to investigate and establish the accuracy of the control system values using Neutron Activation Analysis. This study will ensure the operational safety and obtaining accurate analytical results. The scope of the research is based on validating the neutronic and thermal hydraulic parameters, displayed by the GHARR-1 control system. The reactor was operated at five (5) different power levels and neutron flux data was acquired through Neutron Activation Analysis using Cobalt-60 (^{60}Co) as the flux monitor.

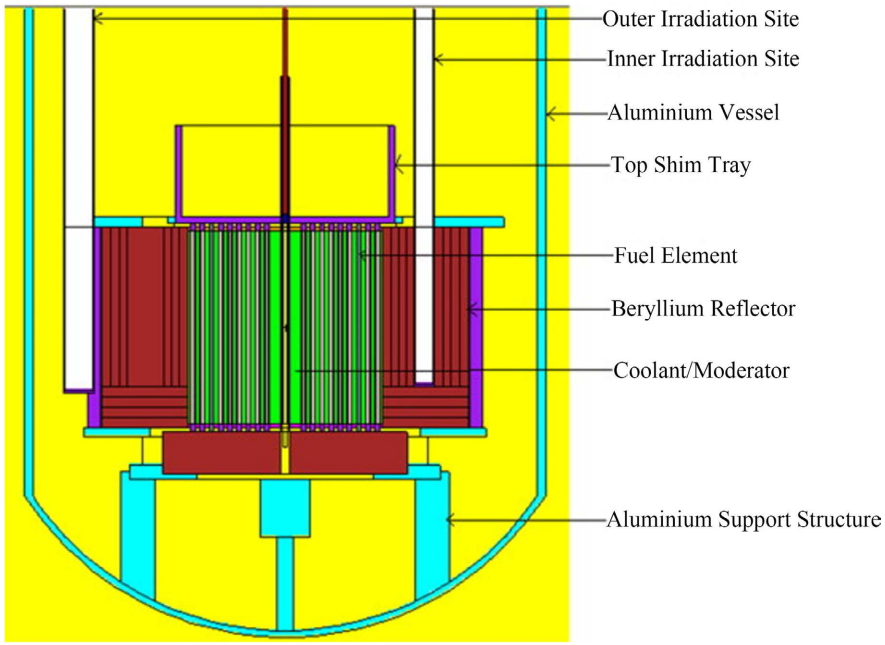

Figure 1. Vertical cross section of the GHARR-1 reactor (Mweetwa *et al.* [2]).

1.1. Measurement of Neutronic and Thermal-Hydraulic Parameters

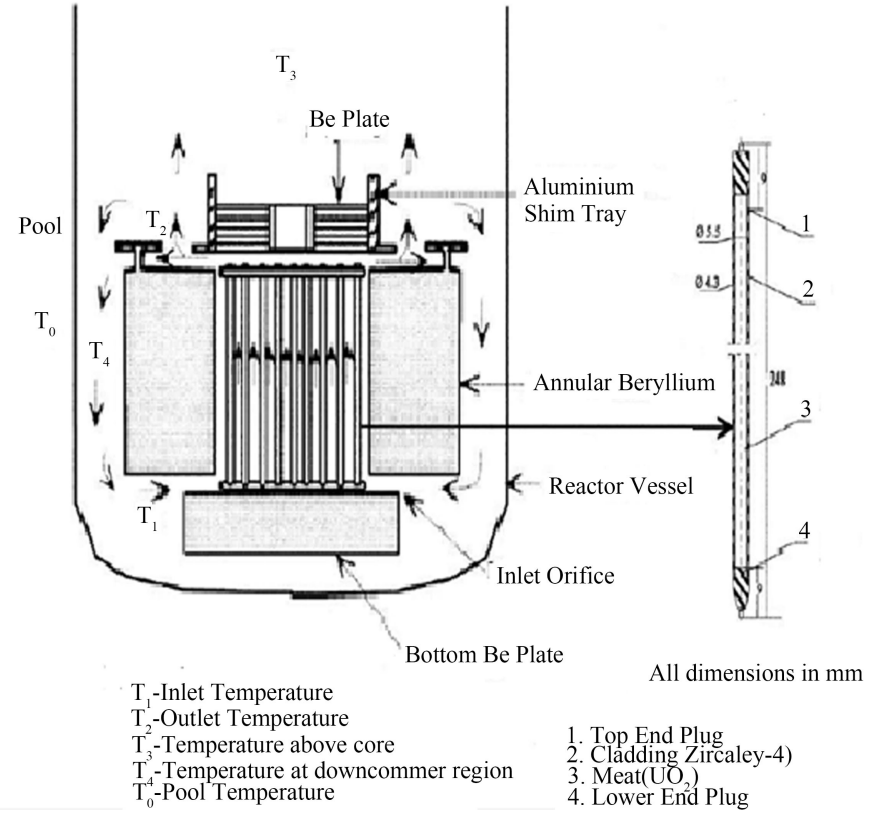

Figure 2. A schematic diagram of the coolant flow pattern in GHARR-1 LEU core (Amoah [11]).

Neutronic and Thermal hydraulic parameters in the reactor core are measured regularly during reactor operation. Thermal neutrons flux is used as the main parameter that indicates the generic performance of a research reactor. By performing a neutronic analysis of the reactor core using the necessary material compositions and geometrical information, one can determine how the distribution of neutron density within the reactor core affects the operations of the reactor. The neutron flux distribution is the main input from which all other core parameters, such as criticality, power, fuel burnup, and fission product poisoning, are derived (Devan & Bachchan [9]). During reactor operation, the thermal-hydraulic characteristics of the reactor are measured using level gauges and thermocouples. The main computer closed loop system is used to monitor the reactor operation (Yamoah *et al.* [10]). The thermal neutron flux was determined using cobalt monitor and the corresponding thermal power was obtained from temperature difference between coolant inlet (T_1) and outlet temperatures (T_2) as shown in **Figure 2**. The control system neutron flux readings were also obtained. In this work, Neutron Activation Analysis method was used to get the flux values, which were compared with the displayed values shown on the control system.

1.2. Neutron Activation Analysis

A sensitive multi-element analytical method called neutron activation analysis (NAA) is used to analyse major, minor, trace, and rare elements both qualitatively and quantitatively. There are two methods used for NAA, which are Destructive Method and Non-Destructive method. The Non-Destructive method was what we implemented in this research (Motimedi *et al.* [12]). The Destructive Method of NAA is when elements of the resulting radioactive sample go through chemical separation and decomposition whilst the non-destructive method first requires activating the sample in a neutron source in order to identify and quantify the induced activity from the concentration of the element in the sample. There are various techniques used to analysed neutron activation analysis such as analytical techniques. Techniques of NAA is grouped into two based on the measurements of gamma rays during neutron irradiation called Prompt Gamma Neutron Activation Analysis (PGNAA) and after radioactive decay is known as Delayed Gamma Neutron Activation Analysis (DGNAA). The PGNAA Technique: is "done by using beam of neutrons extracted through a reactor beam port. Neutron flux on samples that has been irradiated in beams are in order of million times lower than reactor flux. The PGNAA technique is applicable to elements which decay too rapidly with extremely high neutron capture cross-sections like B, Cd, Sm, and Gd, elements that produce only stable isotopes and elements with weak decay gamma-ray" intensities. DGNAA Technique occurs by waiting for the "shorter-lived radionuclide to decay, this technique can improve the sensitivity for a long-lived radionuclide that is hampered by interference from a shorter-lived radionuclide (Baidoo [13]). The physical phenomena upon which NAA is based on are the characteristics of the nucleus, radioactivity, and the interaction of radiation

with matter. Figure 3 depicts the progression of events during a typical (n, y) reaction. A compound nucleus is created in a highly excited state when a neutron collides with a target nucleus in a non-elastic manner. The high neutron-nucleus binding energy is what causes the compound nucleus' high excitation energy, which is 8 MeV on average. Typically, the "lifetime of a compound nucleus ranges from 10^{-16} to 10^{-14} s. This is short enough for the nucleus to undergo a rapid de-excitation to a more stable configuration while being long enough for no traces of the specific formation process to remain. This can happen in a variety of ways, most of which involve the emission of nuclear particles or prompt gamma rays. The new nucleus will typically be radioactive and will continue to de-excite by emitting decay gamma rays. For the purpose of identifying elements and calculating their concentrations in samples, the NAA method depends on the measurement of either these distinctive prompt or decay gamma rays. Approximately 70% of the elements have nuclides with NAA-suitable properties" (IAEA [14]; Alfassi [15]; Chae *et al.* [16]; Jonah [17]; Nyarko *et al.* [18]; Vu *et al.* [19]).

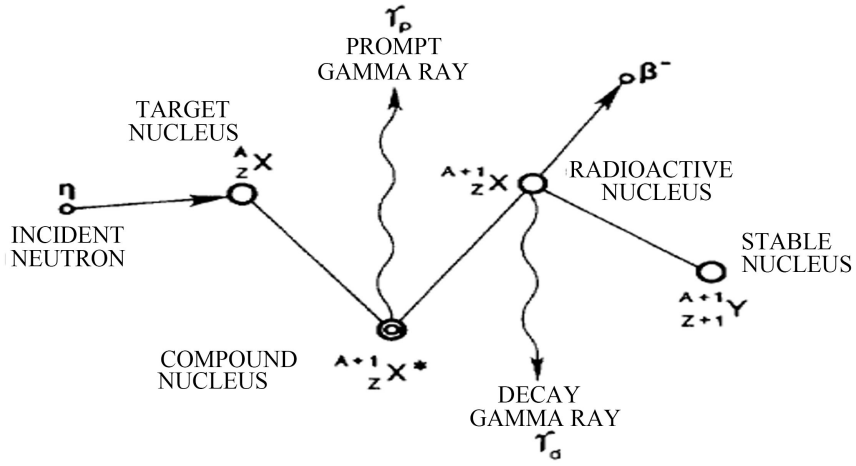

Figure 3. Schematic diagram illustrating the sequence of events for a typical (n, γ) reaction (IAEA [14]).

1.3. Neutron Activation Analysis (NAA) Theory

The analyte's nuclei undergo nuclear processes as a result of neutron irradiation, and the reaction products which are often radioactive emit radiations that can be used to identify and quantify the elements that need to be determined. Among other possibilities of irradiation by charged particles or gamma rays, irradiation by neutrons is the best option since they have no charge and can penetrate the sample more deeply than other options. Neutron interactions can result in the scattering or capture of neutrons to create a composite nucleus. One of these interactions is neutron capture, in which the nucleus absorbs a neutron. The capture of the neutron increases the mass number of the nucleus, thus:

$$X_A^Z + n_0^1 \rightarrow X_A^{Z+1} \quad (1)$$

Neutron activation transforms a nuclide into a new isotope because the isotope

that is produced becomes unstable. While being captured, some neutrons become unstable and go through nuclear transmutation or radioactive decay to become stable (Samaila & Alhji [20]). The reaction rate R per nuclear capturing a neutron is given by

$$R = \int_0^\infty n(v) v \sigma(v) \mathrm{d}v \tag{2}$$

where,

v = neutron velocity (ms^{-1});

$\sigma(v)$ = the neutron cross section in (m^2) with a velocity of v;

$\sigma(v)\mathrm{d}v$ = the density (m^{-3}) of neutrons with velocities between v and $v + \mathrm{d}v$, considered to be constant in time.

While the combined "activation" and "decay" of the isotope during irradiation could be approximated by the expression:

$$\frac{\mathrm{d}N_{A+1}}{\mathrm{d}t} = RN_{0A} - \lambda_{A+1} N \tag{3}$$

Provided the formed nuclide N_{A+1} does nodergo activation as well.

The number of isotope present at the start of measurement is:

$$N_{A+1} = \frac{\varphi \sigma_{0A} N_{0A}}{\lambda_{A+1}} \left[1 - \mathrm{e}^{-\lambda_{A+1} t_i}\right] \mathrm{e}^{-\lambda_{A+1} t_d} \tag{4}$$

where,

φ = reaction neutron flux ($\mathrm{ncm}^2\mathrm{s}^{-1}$);

σ_{0A} = neutron absorption cross section of the original isotope;

$N_{0A} = \dfrac{N_{av} m \theta}{M}$ atomic density of isotope A;

t_i = irradiation time;

t_d = delayed time;

λ_{A+1} = decay constant of the created active isotope.

From the above Equation (4), the right hand side indicates the decay after irradiation and left hand side in the bracket indicates the growth of activity during irradiation (Baidoo [13]).

1.4. Gamma Spectrometry for Neutron Activation Analysis

Figure 4 shows the gamma spectrometry setup. The gamma spectroscopy detectors are made of passive components that allow for interactions to take place in the detector volume. Samples that are exposed to radiation, are then placed within a High Purity Germanium Detector (HPGe) to measure the energy and intensities of the gamma rays. The gamma ray interacts with the detector to generate free-electrons, which is further converted to current, it is then amplified via voltage amplification through preamplifies and then fed into the spectrometry amplifiers which are also known as the main amplifier systems. The main amplifier shapes the current pulses into a Gaussian or trapezoidal shape and it is then fed into the Analogue Digital Converter (ADC). The shaped pulses are converted from analogue to digital numbers. The analogue-to-digital-converter (ADC) have a specific number of "bins" that

sorts the pulses by their height, these bins represent the channels in the spectrum. The Multi-Channel Analyser (MCA) receives the pulses from the ADC. MCA is made up channels which stores the energies and frequencies to a specific channel.

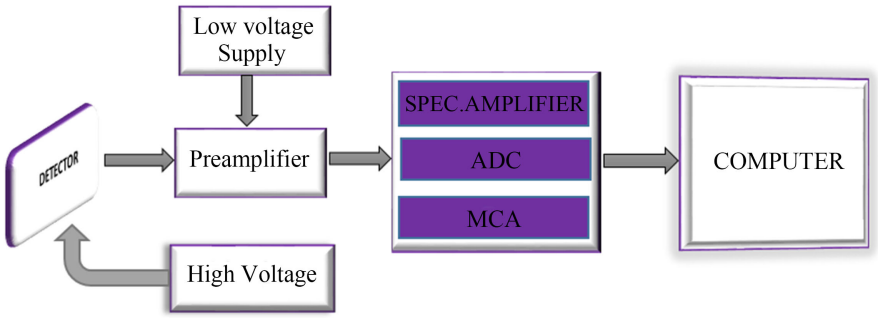

Figure 4. Gamma spectrometry.

1.5. Neutron Activation Reaction Rate

Activation rate of an element is dependent on the cross section (σ) and neutron fluence rate. The reaction rate per nucleus of an isotope under neutron flux is expressed as;

$$R = \int_0^\infty \varphi(E) \cdot \sigma(E) \mathrm{d}E \tag{5}$$

where,

R is in units of [s^{-1}];

$\varphi(E)$ is in units of [$cm^{-2} \cdot s^{-1} \cdot eV^{-1}$];

$\sigma(E)$ in units of [cm^2].

Expressing Equation (5) in equivalent velocity terms thus reaction rate as a function of velocity

$$R = \int_0^\infty \varphi(v) \cdot \sigma(E) \mathrm{d}v \tag{6}$$

where,

$\varphi(v)$ is in units of [cm^{-3}];

E is the energy of the neutron;

v is velocity;

$\sigma(v)$ and $\sigma(E)$ = neutron cross sections with respect to velocity, v and per unit energy at energy, E respectively.

Cobalt was used as the monitor because it has a high fluence rate and monitors thermal neutron fluence in the range of 10^{14} to 10^{18} cm^{-2}. Measurements of thermal neutron flux are commonly carried out with flux monitors of cobalt by the $^{59}Co(n, \gamma)$ ^{60}Co reaction, which has a well-established cross section of 37.1 barns (1 barn = 10^{-24} cm^2) (IAEA [14]).

2. Materials and Methods

2.1. Materials and Equipment

Materials and equipment used for the experiment are as follows:

- Acculab ATL-124 Analytical Scale
- Micro Computer Closed Loop System (MCCLS)
- High Purify Germanium Detectors (HPGe)
- Pneumatic Rabbit System for Sample Delivery
- Flux Monitors; Cobalt (Co)
- Irradiation Capsules

2.2. Acculab ATL-124 Analytical Scale

As seen in Figure 5, the Acculab ATL-124 is an electronic analytical and precision balance with a 120 g weighing capacity. The digital weighing scale has a 120 g tare range and a reading of 1 mg. It consists of both internal and external calibration components, as well as automatic internal calibration functions. The weight of the flux monitor for irradiation was measured using the Acculab ATL-124 analytical scale.

Figure 5. Acculab ATL-124 ANALYTICAL scale.

2.3. High Purity Germanium Detector (HPGe)

The High Purity Germanium Detector (GEM C5970), which is depicted in Figure 6, is a radiation detection device that offers adequate data to identify radionuclides precisely ad consistently from their passive gamma ray emission. The analytical unit is a spectrometry system that uses a 1300-volt bias voltage for the detector and a pre-amplifier to generate an output pulse whose amplitude is proportional to the integrated charge output from the detector. Sequential signal pulses are sorted into parallel amplitude channels using a multichannel pulse height analyser, a main amplifier for amplification, and pulse shaping (Amponsah-Abu *et al.* [21]). The HPGe has a resolution full width half maximum (FWHM) of 1.8 MeV, efficiency of 41% and peak shape (FWTM/FWHM) of 1.88.

The detector makes it possible to evaluate the gamma-ray spectrum in terms of energy. The irradiated flux monitor was positioned on the detector with a geometry of 5.0 cm, and it was counted for 7200 seconds.

Figure 6. Ortec solid-state photon detector.

2.4. Pneumatic Rabbit System for Sample Delivery

For the purpose of sending and retrieving samples, pneumatic systems rely on compressed air (Amponsah-Abu *et al.* [21]). The reactor has ten irradiation channels, five of which are inner channels that can accommodate sample capsules with a volume of 7 cm^3 and are evenly spaced along a concentric circle with a diameter of 330 mm in the side beryllium reflector. Outside of the beryllium annulus, five outside irradiation tubes have been erected. The pneumatic system was utilized to move the flux monitors into the reactor core's inner irradiation site "A".

2.5. Cobalt (Co) Flux Monitors

Cobalt aluminium alloy wire of 0.5 mm diameter was used as a flux monitor because of its high fluence rate (**Figure 7**). It monitors thermal neutron fluence in the range of 10^{14} to 10^{18} cm^{-2}. It has a half-life of 1925.5 days. The neutron reaction involved is $^{59}Co(n, \gamma)\ ^{60}Co$. Two gamma rays with energies of 1.17 and 1.33 MeV are released by ^{60}Co (Vigneshwara Raja *et al.* [22]).

Figure 7. Cobalt wire.

2.6. Preparation of Flux Monitor

The flux monitors with masses ranging from 15 mg to 85 mg were put into a polyethylene capsule (smaller capsule). The capsules were then placed in a bigger capsule and the space left on top was tightly filled with cotton wool for it to be airtight. The flux monitors were prepared in this same manner for all the irradiations at the different power levels from 0.17 kW to 34 kW.

2.7. Irradiation Capsules

Irradiation capsules are made up of polyethylene that is used to shield the flux monitors presented in Figure 8. Dimensions of capsules used:

- Big cylindrical polyethylene capsule height = 5.55 cm
- Inner diameter = 1.5 cm
- Outer diameter = 1.65 cm
- Small cylindrical polyethylene capsule, height = 2.35 cm
- Inner diameter = 1.05 cm
- Outer diameter = 1.2 cm

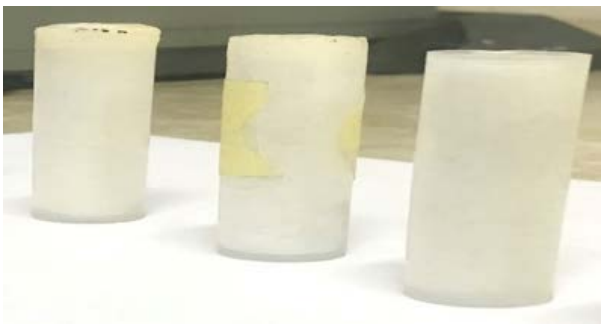

Figure 8. Polythene capsules.

2.8. Methods

At the inner irradiation site "A" of the GHARR-1 reactor core, where highest fluxes were observed, the neutronic and thermal-hydraulic parameters were measured. The neutron flux, inlet temperature, outlet temperature, and the temperature difference across the core were monitored while the reactor was run at five (5) different power levels ranging from 0.17 kW to 34 kW. The cobalt monitors were analysed using Neutron Activation Analysis (NAA) method and the outcomes were compared with the pre-set and measured neutron flux values acquired from the control system's computer, the Micro Computer Close Loop System (MCCLS).

2.9. Detector Calibrations

Calibration is set of adjustment made on an instrument to make that instrument functions accurately. Calibration is done to maintain standardization and reproducibility of measurements, assuring reliable benchmarks and results. To identify radio nuclides within a radioactive source at the same time to determine their

complete activity, it is important to discriminate the emitted γ-quanta with respect to their energies which is known as γ-spectrometry. The γ-spectrometry is performed with either sodium iodide (NaI) or germanium detectors (Baidoo [13]). Detector efficiency is a measurement of how much radiation a certain detector can detect out of the total amount of radiation emitted by the source (Akkurt *et al.* [23]). Detector efficiency is divided into two types, total efficiency and peak efficiency. Total efficiency indicates the probability that a quantum or photon incident on the detector will result in a pulse of any magnitude. Peak Efficiency is the likelihood that the quantum will completely expend its original energy in the detector's active volume.

Multi-line gamma-ray standards that cover the relevant energy range are typically used to achieve the efficiency calibration curve of intrinsic germanium (HPGe) detectors for spectrometric study of gamma-ray emitters. The nine-radio nuclide mixture of the most popular multiline gamma-ray standards consists of ^{241}Am, ^{109}Cd, ^{57}Co, ^{139}Ce, ^{203}Hg, ^{113}Sn, ^{137}Cs, ^{88}Y and ^{60}Co were used for the calibration.

2.9.1. Efficiency Calibration

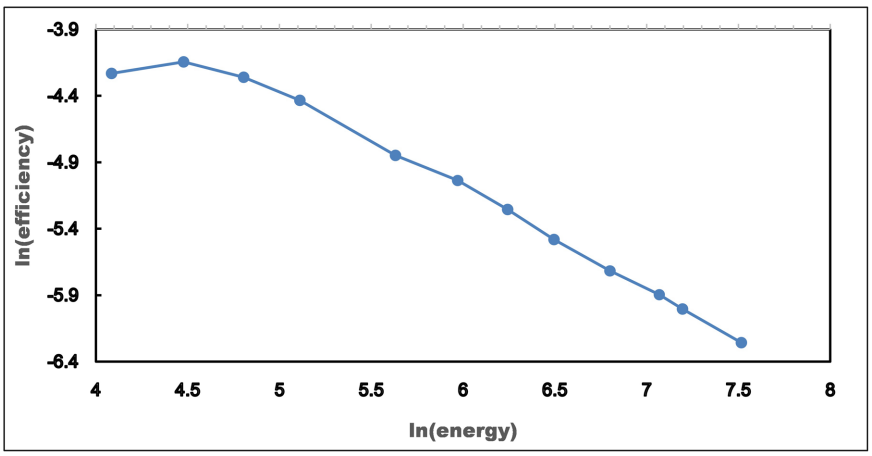

Figure 9. Efficiency calibration curve.

The efficiency calibration of the detector is carried on to ensure the efficient operation of the detector. A radioactive source emits a certain number of photons (gamma radiation) and the detector (HPGe detector) is used to detect these photons. The number of photons emitted by the radioactive source is always larger than the number of photons observed by the detector, and the ratio of the number of photons detected or observed by the detector with respect to the number of photons emitted by the source is known as the detection efficiency. The efficiency calibration was obtained using High Purity Germanium Detector (HPGe) at different geometries within the energy range of 53.16 to 1408 keV. Monitors used are (^{137}Cs) and multi (^{60}Co, ^{133}Ba, ^{152}Eu and ^{241}Am) gamma ray emitters. Counting time was prolonged to ensure at least 95% statistical significance curve. The efficiency was measured at various source-to-detector distances. The efficiency calibration

curve is a plot of the efficiency against energy. Figure 9 shows the efficiency calibration curve.

2.9.2. Energy Calibration

The primary significance of calibration is that it maintains accuracy, standardization and repeatability in measurements, assuring reliable benchmarks and results. Without regular calibration, equipment can fall out of specifications, provide inaccurate measurements and threaten quality. The energy calibration is done to determine the relationship between the energy of a gamma ray and the centroid channel number of the peak produced by that gamma ray. The source used to perform the energy calibration is ^{60}Co, which emits gamma rays of known energy (1173.2 keV, 1332.5 keV). On the cap of the detector, ^{60}Co was placed at the same geometry as the samples. The peaks from the lowest channel to the highest channel were found via statistical counting for at least 300 sec. The Gamma Vision spectrums with the ^{60}Co peaks were chosen for calibration. The plot of gamma ray energy as a function of channel number is known as the energy calibration curve.

Figure 10 shows the energy calibration curve of the detector.

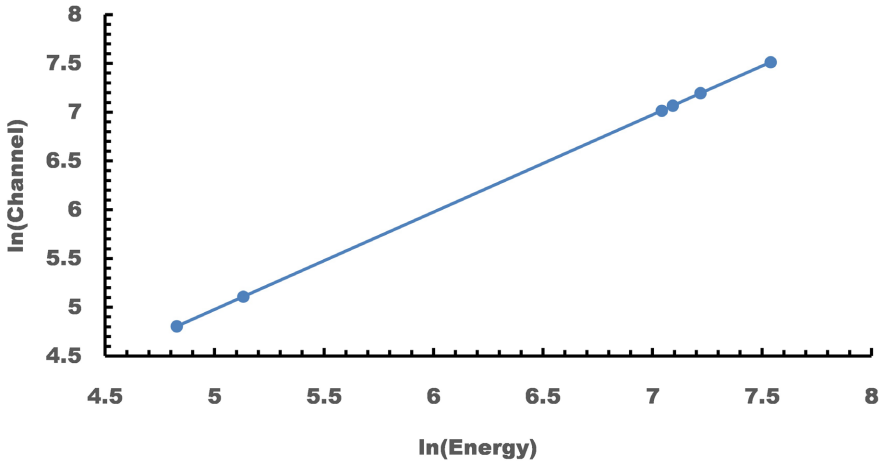

Figure 10. Energy calibration curve.

2.10. Temperature and Neutron Flux Measurement

GHARR-1 was operated at five different power levels; 0.17 kW, 10.2 kW, 17 kW, 27.2 kW and 34 kW, using the Micro Computer Close Loop Systems (MCCLS). Reactor was operated at these power levels. Thermal hydraulics and neutronic parameters were recorded at these power levels. These parameters include inlet and outlet temperatures, control rod position, and neutron fluxes at different power levels. The instruments used in measuring thermal hydraulic parameters are thermocouples and the neutronic parameter was determined via the fission chamber within the reactor core.

2.11. Irradiation, Counting and Interpretation of Flux Monitor

Flux monitors were irradiated at reactor power levels of 0.17 kW, 10.2 kW, 17 kW,

27.2 kW, and 34 kW which corresponds to neutron flux levels 5.0×10^9, 3.0×10^{11}, 5.0×10^{11}, 8.0×10^{11} and 1.0×10^{12} $ncm^{-2} \cdot s^{-1}$ respectively. Each monitor was irradiated for a maximum of 3 hrs except the monitor which was irradiated at full power (34 kW) for 1 hr 30 min and was allowed to decay a day before data collection was made on the High Purity Germanium detector for 7200 seconds. The gamma spectrum obtained from the irradiation was allowed to be interpreted by gamma vision software which is able to calculate all the flux parameters at a single command for interpretation. Counting of the emitted gamma rays were achieved by using High Purify Germanium Detector, with an efficiency of 41% and a resolution at 1.8 KeV. The detector was connected to a DSPEC jr 2.0 digital signal processing gamma ray Spectrometer with Maestro 32 spectroscopy software for the acquisition of spectra.

2.12. Characterization of the Flux Monitor

Generally, in NAA the mass of the flux monitors analyzed ranges from 10.0 mg to 40.0 mg and the values measured are used in the computation of the fluxes. Also, the weight of the fluxes can be varied since characterization does not depend on the weight. Each monitor was inserted into different capsules labelled according to their power levels and was irradiated between one and half hour to three hours. With a percentage purity of 0.1% the actual mass of cobalt can be determined using the equation below:

$$\text{The actual mass of a sample} = \frac{\text{Total mass weighed}}{100\%} \times (\%\ \text{Purity})$$

The percentage compositions of each monitor calculated is shown below in Table 1:

Table 1. Composition of cobalt monitors and respective weights.

Power Levels	Weight/Mass (mg)	% Purity
34.0 kW	0.0152	0.1
27.2 kW	0.0261	0.1
17.0 kW	0.0085	0.1
10.2 kW	0.0133	0.1
170.0 W	0.0183	0.1

2.13. Reactor Fission Power Based on Neutronics and Thermal-Hydraulic Parameters

Equation (8) and Equation (11) respectively, illustrate the steady and transient states where the correlation between temperature and power and the interaction between neutron flux and power, were studied. As a result, the calculation of the reactor's fission power using neutronic parameters is given by Equation (7):

$$P = 3.4 \times 10^{-10} \Sigma_f V_f \phi \tag{7}$$

where ϕ = average thermal neutron flux in the inner irradiation channel

(n/cm^{2}s);

V_f = Volume of the core = $\Pi r^2 h$ (cm^3);

Core height (h) = 23 cm;

Core radius (r) = 11.55 cm;

$\Sigma_f = N_f$ (microscopic fission cross section of the core = 1.013×10^{-2} cm^{-1}).

Substituting Volume, height and radius of the core into Equation (7) gives Equation (8)

$$P = 3.4 \times 10^{-8} \phi \tag{8}$$

2.14. Measurement of Thermal Hydraulic Parameters of MNSR

Heat is removed from the core by natural convection. Safety testing shows that for the thermal hydraulics design of the MNSR to achieve the required rise in temperature, the height of the input orifice must remain at 6 mm and the output at 7 mm. These design requirements formed the foundation for the relationship between coolant temperature and reactor power (Amponsah-Abu [3]). The input temperature, coolant temperature rise, and power levels have the following semi-empirical connection, according to MNSR tests (Amponsah-Abu [3]):

$$\Delta T = \left(5.725 + 147.6 H^{-2.64}\right) T_i^{-0.35} P^{0.59+0.0019 T_i} \tag{9}$$

where,

ΔT = Temperature difference between inlet and outlet orifice (˚C);

H = Height of the inlet orifice given as 6 mm;

T_i = Inlet temperature (˚C);

P = Power (kW).

Putting H into Equation (9) gives:

$$\Delta T = \left(6.81 T_i^{-0.35}\right) P^{0.59+0.0019 T_i} \tag{10}$$

Hence, the correlation for power and temperature difference across the core.

From Equation (10), calculating for the correlation power (P).

$$P = \exp\left[\ln\left(\frac{\Delta T}{6.81 T_i^{-0.35}}\right)\left(0.59 + 0.0019 T_i\right)^{-1}\right] \tag{11}$$

2.15. Determination of Thermal Neutron Fluence

Cobalt was used in this study to calculate the thermal fluence rate. It is possible to compute the following for a tiny sample of radioactive cobalt:

$$\phi_0 = \frac{R_s}{g \sigma_0} \tag{12}$$

where:

R_s = reaction rate per target atom;

σ_0 = Thermal cross section (2200 m/s);

g is the modification factor for thermal region cross-section deviation of the detecting foil from $1/v$ cross-section behavior.

The reaction rate is given by

$$R_s = \frac{C\exp(\lambda t_w)}{\varepsilon N_0\left(1-\exp(-\lambda t_i)\right)} \tag{13}$$

where,

R_s = reaction rate per target atom;

C = Net counting rate of cobalt in the sample at the time of measurement;

λ = Decay constant corresponding to half-life of 1925.5 days;

N_0 = Original number of atoms of nuclide to be activated (given by the product of the weight in grams of the ^{60}Co and Avogadro's number divided by the atomic weight of the element in grams);

ε = Efficiency of the detector;

t_i = Exposure duration;

t_w = Time elapsed from the end of exposure period to the time of counting.

When the exposure time is small,

$$1-\exp(-\lambda t_i) \approx \lambda t_i \tag{14}$$

Hence, Equation (12) becomes:

$$\phi_0 = \frac{C\exp(\lambda t_w)}{\lambda t_i N_0 \varepsilon \sigma_0} \tag{15}$$

The Equation (15) is the equation used for the calculation of fluence (neutron flux) for cobalt monitor over the irradiation period [3] [13].

3. Results and Discussion

This section presented and discussed neutronic and thermal hydraulics results obtained from the study using GHARR-1 LEU.

3.1. Criticality Results

The reactor was operated at the critical power of 170 Watts corresponding to a neutron flux of 5.0×10^9 n/cm^{2}s. **Figure 11** shows the graph of core excess reactivity against control rod position at critical rod positions. The graph is used to determine the reactivity of the core after a long period of operation in order to determine whether to add beryllium shims. Beryllium shims are only added when the reactivity falls below 3.5 mk. This is to optimized neutron economy in the core.

During the commissioning of the reactor, 3.87 mk core reactivity was experimentally determined at 93.6 mm control rod height at a critical flux of 5×10^9 n/cm^{2}s (Li *et al.* [24]). For this work, the control rod height of 100 mm was recorded corresponding to an excess reactivity of 3.6 mk, indicating a decrease in reactivity but it is still within the range of 3.5 mk to 4.0 mk as specified in the Safety Analysis Report (SAR) for GHARR-1. The shutdown margin corresponding to the excess reactivity of 3.6 mk is 3.3 mk (the shutdown margin is the difference between the control rod worth of 6.9 mk and the excess reactivity of 3.6 mk).

The shutdown margin should not be less than 2.5 mk for GHARR-1 MNSR. Base on this result, the experimental work was carried out.

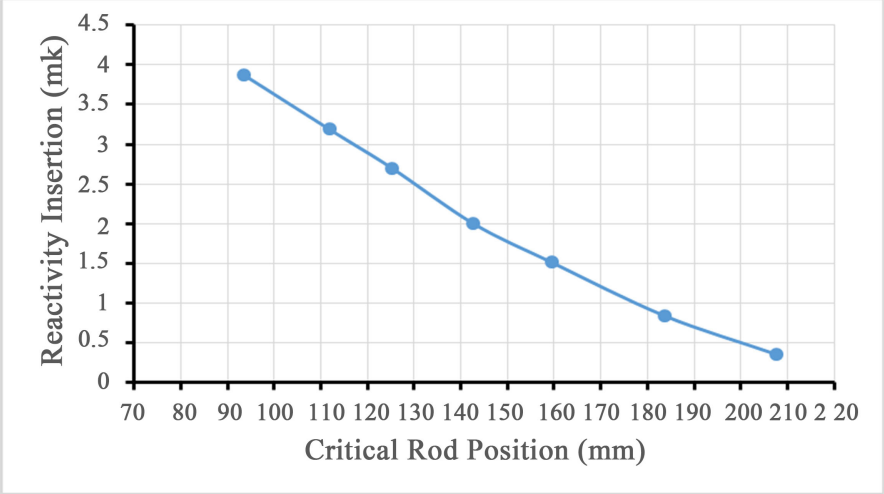

Figure 11. Core excess reactivity graph.

3.2. Experimental Results of Thermal Neutron Flux Measurements

The flux calculated using the Neutron Activation Analysis with flux monitors and the reading on the MCCLS are compared in Table 2. The findings showed marginal differences in the flux levels between the MCCLS values and the measured values.

Table 2. Comparison of neutron flux reading on the MCCLS with the experimental neutron flux using flux monitor at various powers.

Thermal Power (kW)	Average Thermal Neutron Flux Reading on the MCCLS ($ncm^{-2}s^{-1}$)	Experimental Values using flux monitor ($ncm^{-2}s^{-1}$)	Percentage deviation in neutron flux values %	Mean Deviation in % of neutron flux values
0.17	4.99E+09	4.82E+09	3.4	
10.2	3.00E+11	2.89E+11	3.6	
17.0	4.99E+11	4.63E+11	7.2	5.3
27.2	8.00E+11	7.40E+11	7.5	
34.0	9.98E+11	9.50E+11	4.8	

The results shown in Table 2 indicate variations in the flux values between what was measured using activation method and those recorded on the MCCLS. However, it can also be seen that measurement by the activation method were systematically lower than those recorded on the MCCLS. The findings demonstrate that the neutron fluxes displayed on the MCCLS are 1.08 times greater than the neutron fluxes observed using a flux monitor at the inner irradiation site of the reactor while the reactor was run at the various power levels.

After operating the reactor at the critical neutron flux of 5.0×10^9 n/cm^2s, the average percentage of flux deviation from the actual pre-set and displayed values

was 5.3% for the past 5 years of operation and decrease in reactivity from 3.87 mk to 3.6 mk. The monitor neutron flux deviation might be attributed to errors resulting from γ-decay correction factors, self-shielding factor and γ-ray decay branching factor as well as detector efficiency calculation error.

3.3. Comparison between Pre-Set Reading and Mean MCCLS Reading

Pre-set flux is the value of flux inputted vis-à-vis the actual flux in the core displayed on the MCCLS.

From the MCCLS, it was observed that there was not much variation from the MCCLS readings and the pre-set readings as shown in Figure 12 and Table 3. Values determined were approximately equal to the pre-set values, about 0.2% deviation. The values of the commissioning report (Li *et al.* [24]) are consistent with the findings of the current study. The importance of this graph is to verify and establish the accuracy of the GHARR-1 MCCLS displayed parameter values as per the study objectives. The neutron flux values (reactor power) display by the MCCLS should be approximately the same as the pre-set value.

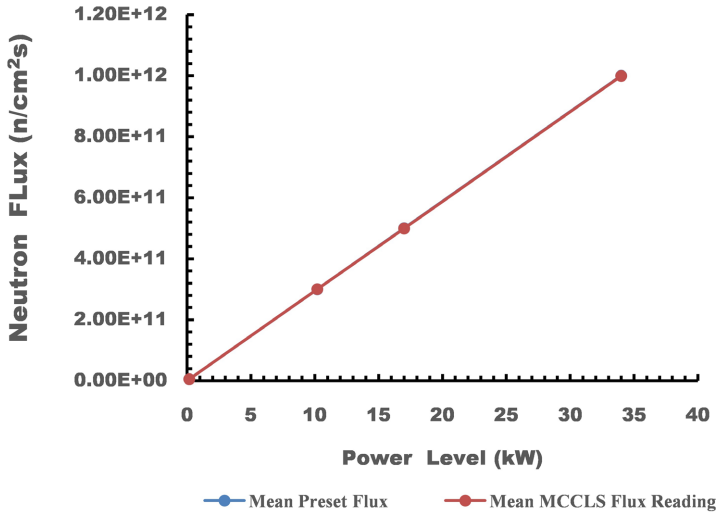

Figure 12. Variation of pre-set values against mean MCCLS reading.

Table 3. Comparison between MCCLS readings and the pre-set values.

Pre-set Thermal Power (kW)	Pre-set Neutron Flux ($ncm^{-2}s^{-1}$)	Mean MCCLS Meter Flux reading ($ncm^{-2}s^{-1}$)	Variation in neutron Flux values (%)
0.17	5.0E+09	4.99E+09	0.2
10.2	3.0E+11	3.00E+11	0.0
17.0	5.0E+11	4.99E+11	0.2
27.2	8.0E+11	8.00E+11	0.0
34.0	1.0E+12	9.98E+11	0.2

Table 3 shows comparison between MCCLS readings and the pre-set values.

The corresponding percentage difference between MCCLS readings and the pre-set values are also provided in the table. There is insignificant difference between MCCLS readings and the pre-set values.

3.4. Variation of Pre-Set Flux Levels with Temperature Readings from MCCLS

Variation of pre-set neutron flux values against reactor temperature values reported by the control system is depicted in Figure 13 (MCCLS). According to reading trends, temperature rises in direct proportion to reactor power (neutron flux). The temperatures at the inlet and outlet increased gradually over time. This is as a result of the core's compact structure, which was intended to prevent adequate coolant thermal circulation. The MCCLS reading shows the linearity and the reliability of the control system. The trend of Figure 13 shows that approaching full power of 34 kW, the negative temperature of reactivity is very high causing high xenon poison effect as temperature increases.

The graphs' general trend demonstrates that the control rod position steadily increases over time to account for the significant negative temperature coefficient of reactivity and maintain the reactor at the specified power levels.

The temperature difference across the core and the inlet temperature were used to calculate the thermal hydraulic power in Equation (11).

Figure 13 compares variation of neutron flux levels with the inlet temperature, outlet temperature and temperature difference across the core during operation.

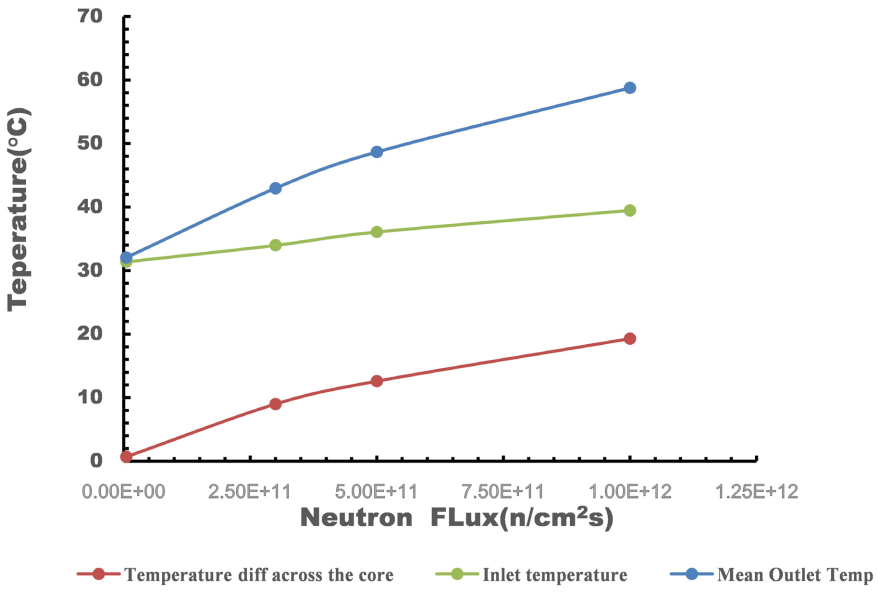

Figure 13. Variation of neutron flux levels with inlet, outlet and temperature difference across the core.

3.5. Variation of Pre-Set Power Levels and Power Calculated from In-Let and Out-Let Temperature Difference (Predicted Power)

Figure 14 below shows variations of predicted power (using temperature and

power correlation) against pre-set power levels. To get the desired power levels, the inlet temperatures and the temperature difference across the reactor core were entered into the power correlation Equation (11). The experimental thermal hydraulics results obtained shows a variation in the predicted power levels as compared with the pre-set power levels giving a mean variation of 5.8%. This is an indication of the reduction of the reactivity of the core, from 3.87 mk to 3.6 mk.

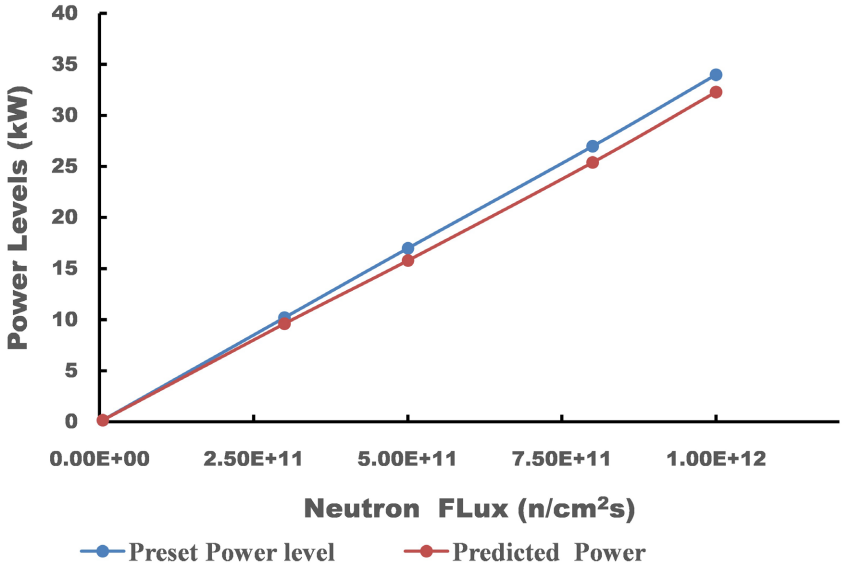

Figure 14. A graph of predicted power against pre-set power level.

3.6. Variation of Pre-Set Power and Activation Calculated Power

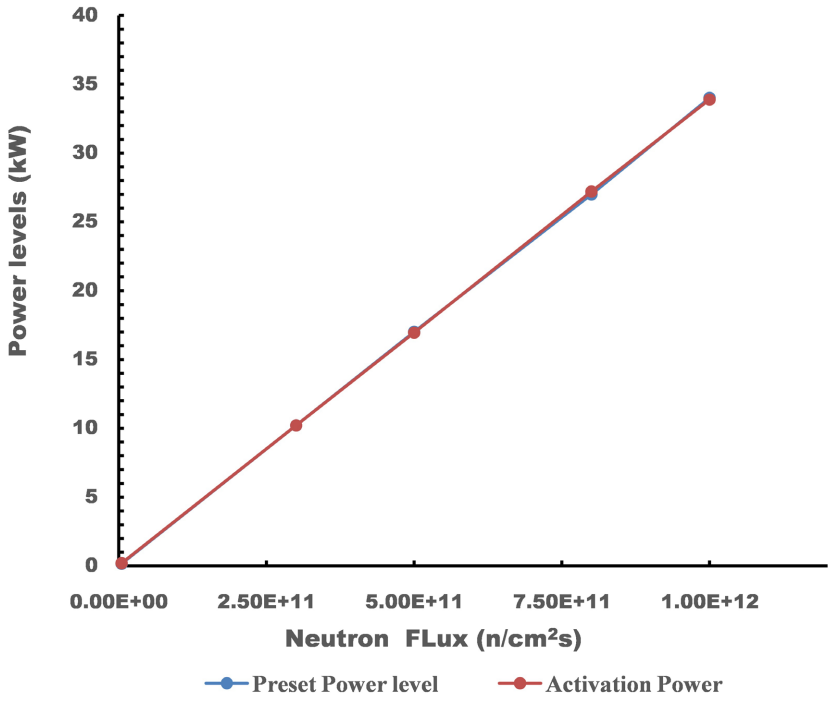

Figure 15. A graph of pre-set power against activation calculated power.

Figure 15 indicates variation of activation power values against pre-set power levels. The fluxes obtained from the experiment (NAA) were inserted into Equation (8) for the Activation Power. The variation between the two powers was calculated to be 0.2%. The 0.2% variation is within the MCCLS acceptable range of ±1.0%. This means that the control system is reliable for operation.

4. Conclusions

The accuracy of neutronic and thermal hydraulic measurement values displayed by the Ghana Research Reactor-1 (GHARR-1) control system was investigated. The reactor core underwent a conversion from High Enriched Uranium (HEU) to low Enriched Uranium (LEU). After five (5) years of operation with the new LEU core, it is necessary to validate the core parameters of the reactor if it is safe to continue operation.

The control rod height during the commissioning at critical flux (power) of 5.0 $\times$ 10^9 n/cm^{2}s equivalent to 170 W at almost zero temperature change across the reactor core was 93.6 mm, which is associated with 3.87 mk core excess reactivity. The control rod height after operating for 545 hours within five (5) years, gave an average control rod height of 100 mm equivalent to 3.6 mk using the core excess reactivity graph of control rod height against core excess reactivity.

Using the flux monitor (cobalt) at the central irradiation site of the reactor, the average percentage deviations of the fluxes obtained in comparison with the preset values of $5.0 \times 10^9 - 1.0 \times 10^{12}$ n/cm^{2}s were 5.3%. The deviation is attributed to the reduction in core excess reactivity from 3.87 mk to 3.6 mk. The results obtained with regards to the thermal-hydraulics (using inlet and outlet temperature reading in the core) showed a 5.8% variation in the thermal-hydraulics experimental power levels compared with the displayed preset power levels.

Analysing the results from both methodologies of using flux monitor and inlet-outlet temperature readings, the margin between the experimental flux monitor and the thermal-hydraulic flux results is minimal; this is an indication that after 5 years of operating the reactor, it is safe to continue operation.

Conflicts of Interest

There is no conflict of interest between the results obtained from this study and similar study results obtained in literature.

References

[1] Amusai, J.H., Schandorf, C. and Yeboah, J. (2001) Safety of Ghana Research Reactor (GHARR-1) (IAEA-CN-82). International Atomic Energy Agency (IAEA), 1-4.

[2] Mweetwa, B.M., Ampomah-Amoako, E., Akaho, E.H.K. and Odoi, C. (2018) Prediction of Neutronic and Kinetic Parameters of Ghana Research Reactor 1 (GHARR-1) after 19 Years of Operation Using Monte Carlo-N Particle (MCNP) Code. *World Journal of Nuclear Science and Technology*, **8**, 160-175. https://doi.org/10.4236/wjnst.2018.84014

[3] Amponsah-Abu, E.O. (2013) Assessment of the Reliability of Thermal-Hydraulic and

Neutronics Parameters of Ghana Research Reactor-1 Control Systems. Ph.D. Thesis, University of Ghana.

[4] Amoah, P., Shitsi, E., Ampomah-Amoako, E. and Odoi, H.C. (2020) Transient Studies on Low-Enriched-Uranium Core of Ghana Research Reactor-1 (GHARR-1). *Nuclear Technology*, **206**, 1615-1624. https://doi.org/10.1080/00295450.2020.1713681

[5] Amponsah-Abu, E.O., Gbadago, J.K., Akaho, E.H.K., Akoto-Bamford, S., Gyamfi, K., Asamoah, M., *et al.* (2015) Assessment of the Reliability of Neutronic Parameters of Ghana Research Reactor-1 Control Systems. *Nuclear Engineering and Design*, **281**, 72-78. https://doi.org/10.1016/j.nucengdes.2014.11.018

[6] Baidoo, I.K., Nyarko, B.J.B., Akaho, E.H.K., Dampare, S.B., Sogbadji, R.B.M. and Poku, L.O. (2013) Characterization of Low Power Research Reactor Neutrons for the Validation of k_0-INAA Standardization Based on k_0-IAEA Software. *Applied Radiation and Isotopes*, **79**, 85-93. https://doi.org/10.1016/j.apradiso.2013.05.005

[7] Osei, B. (2017) Characterization of Ghana Research Reactor-1 Low Enriched Uranium Core Irradiation Sites Using a Theoretical Method. Ph.D. Thesis, University of Ghana.

[8] Osei, B., Baidoo, I.K., Odoi, H.C., Gasu, P.D. and Nyarko, B.J.B. (2021) The Low Enriched Uranium Miniature Neutron Source Reactor (LEU-MNSR) Neutron Spectrum Characterization for k_0-INAA. *Nuclear Instruments and Methods in Physics Research Section A*: *Accelerators*, *Spectrometers*, *Detectors and Associated Equipment*, **1005**, Article ID: 165397. https://doi.org/10.1016/j.nima.2021.165397

[9] Devan, K. and Bachchan, A. (2021) Homogeneous Reactor and Neutron Diffusion Equation. In: Mohanakrishnan, P., Singh, O.P. and Umasankari, K., Eds., *Physics of Nuclear Reactors*, Elsevier, 193-262. https://doi.org/10.1016/b978-0-12-822441-0.00004-2

[10] Yamoah, S., Akaho, E.H.K., Nyarko, B.J.B., Asamoah, M., Ampong, A.G. and Amponsah-Abu, E.O. (2011) Analysis of Thermal-Hydraulic Transients for the Miniature Neutron Source Reactor (MNSR) in Ghana. *Research Journal of Applied Sciences*, *Engineering and Technology*, **3**, 737-745.

[11] Amoah, P. (2019) Thermal Hydraulic Analysis of Low Enriched Uranium (Leu) Core of the Ghana Research Reactor-1 (GHARR-1). Ph.D. Thesis, University of Ghana.

[12] Motimedi, T., Vilakazi, H., Thoane, K., Adamchyk, D., Lapatsentava, T., Petrov, A. and Govor, E. (2011) Instrumentan Neutron Activation Analysis (INAA). Frank Laboratory of Neutron Physics Summer Practice, JINR-DUBNA, 1-20.

[13] Baidoo, I.K. (2012) Validation of IAEA k_0-Instrumental Neutron Activation Analysis Software Using Low Power Research Reactor. Ph.D. Thesis, University of Ghana.

[14] IAEA (1990) Practical Aspects of Operating a Neutron Activation Analysis Laboratory. International Atomic Energy Agency (IAEA), IAEA-TECDOC-564.

[15] Alfassi, Z.B. (2000) Instrumental Neutron Activation Analysis. In: Meyers, R.A., Ed., *Encyclopedia of Analytical Chemistry*, Wiley, 12497-12526.

[16] Chae, S., Lee, J. and Kim, Y. (2021) Neutron Diagnostics Using Nickel Foil Activation Analysis in the KSTAR. *Nuclear Engineering and Technology*, **53**, 3012-3017. https://doi.org/10.1016/j.net.2021.03.021

[17] Jonah, S.A., Ibrahim, Y.V., Ajuji, A.S. and Onimisi, M.Y. (2012) The Impact of HEU to LEU Conversion of Commercial MNSR: Determination of Neutron Spectrum Parameters in Irradiation Channels of NIRR-1 Using MCNP Code. *Annals of Nuclear Energy*, **39**, 15-17. https://doi.org/10.1016/j.anucene.2011.08.026

[18] Nyarko, B.J.B., Akaho, E.H.K. and Serfor-Armah, Y. (2003) Application of NAA

Standardization Methods Using a Low Power Research Reactor. *Journal of Radioanalytical and Nuclear Chemistry*, **257**, 361-366.
https://doi.org/10.1023/a:1024744131848

[19] Vu, C.D., Thein, T.Q., Doanh, H.V., Quyet, P.D., Anh, T.T.T. and Dien, N.N. (2014) Characterization of Neutron Spectrum Parameters at Irradiation Channels for Neutron Activation Analysis after Full Conversion of the Dalat Nuclear Research Reactor to Low Enriched Uranium Fuel. *Nuclear Science and Technology*, **4**, 70-75.
https://doi.org/10.53747/jnst.v4i1.216

[20] Samaila, B. and Alhji, S.A. (2020) Scientific Review on Theory and Mechanism of Neutron Activation Analysis in Geological and Environmental Samples. *International Journal of Mathematics and Physical Sciences Research*, **7**, 87-100.

[21] Amponsah-Abu, E.O., Nyarko, B.J.B. and Edziah, R. (2019) Design and Construction of Pneumatic Transfer System Controller Unit for Ghana MNSR. *Journal of Control Science and Engineering*, **2019**, Article ID: 6450987.
https://doi.org/10.1155/2019/6450987

[22] Vigneshwara Raja, P., Rao, C.V.S. and Narasimha Murty, N.V.L. (2016) Numerical Simulation of ^{60}Co-Gamma Irradiation Effects on Electrical Characteristics of N-Type FZ Silicon X-Ray Detectors. *Nuclear Instruments and Methods in Physics Research B*, **379**, 23-27. https://doi.org/10.1016/j.nimb.2016.04.052

[23] Akkurt, I., Gunoglu, K. and Arda, S.S. (2014) Detection Efficiency of NaI(TL) Detector in 511-1332 Kev Energy Range. *Science and Technology of Nuclear Installations*, **2014**, Article ID: 186798. https://doi.org/10.1155/2014/186798

[24] Li, Y., Peng, D., Lu, J., Wu, X., Hong, J., Hao, Q., Wang, M., Odoi, H.C., Aboh, I.J.K., Amponsah-Abu, E.O., Aboh, I.J.K., Ofosu, F.G., Gyamfi, K., Osei-Mensah, W., Shitsi, E., Ampong, A.G., Quagraine, R.E., Obeng, H.K., Gasu, P.D. and Osei, B. (2017) Report for GHARR-1 Loading of LEU Core and Commissioning, National Nuclear Research Institute, Ghana Atomic Energy Commission, Kwabenya, Accra-Ghana.